

**Low-temperature anisotropic magnetoresistance and planar Hall effect in SrRuO<sub>3</sub>**Noam Haham,<sup>1,\*</sup> Yishai Shperber,<sup>1,\*</sup> James W. Reiner,<sup>2</sup> and Lior Klein<sup>1</sup><sup>1</sup>*Department of Physics, Nano-magnetism Research Center, Institute of Nanotechnology and Advanced Materials, Bar-Ilan University, Ramat-Gan 52900, Israel*<sup>2</sup>*HGST, 3403 Yerba Buena Rd, San Jose, California 95315, USA*

(Received 4 January 2013; revised manuscript received 7 March 2013; published 9 April 2013)

SrRuO<sub>3</sub> is an itinerant ferromagnet with a Curie temperature of 150 K and a uniaxial magnetocrystalline anisotropy. Using high-quality epitaxial thin films, we measure at 2 K the anisotropic magnetoresistance and the planar Hall effect as a function of the in-plane current direction and the magnetization orientation. We identify three types of contributions related to (a) the orientation of the magnetization relative to the crystal axes, (b) the direction of the current relative to the crystal axes, and (c) the orientation of the magnetization relative to the current.

DOI: [10.1103/PhysRevB.87.144407](https://doi.org/10.1103/PhysRevB.87.144407)

PACS number(s): 75.47.-m, 72.25.Ba, 75.50.Cc, 72.15.Gd

**I. INTRODUCTION**

The interplay between magnetism and electrical transport in the presence of spin orbit coupling gives rise to anisotropic magnetoresistance (AMR) and planar Hall effect (PHE) corresponding to effects on the longitudinal and transverse resistivities ( $\rho_{xx}$  and  $\rho_{xy}$ ), respectively. For polycrystalline magnetic conductors the AMR and PHE are determined only by the angle between the current direction and the magnetization ( $\phi$ ), and dependencies of the AMR and the PHE on the orientation of the magnetization and the current relative to the crystal axes are averaged out. The AMR and PHE are commonly described by<sup>1</sup>

$$\rho_{xx} = \rho_1 + \Delta\rho \sin^2 \phi \quad (1)$$

$$\rho_{xy} = \frac{1}{2} \Delta\rho \sin 2\phi, \quad (2)$$

where  $\Delta\rho$  and  $\rho_1$  are constants.

In crystalline magnetic conductors, the AMR and PHE may include other terms allowed by symmetry,<sup>2</sup> as it has been recently demonstrated for epitaxial thin films of manganites and magnetites.<sup>3</sup> The AMR and PHE of epitaxial thin films of the itinerant ferromagnet SrRuO<sub>3</sub><sup>4</sup> are particularly interesting for the large spin orbit coupling and the fact that the direction of the easy axis of magnetization below the Curie temperature does not coincide with any of the crystal axes. The AMR and PHE of thin films of SrRuO<sub>3</sub> have been studied in the paramagnetic phase where the easy axis coincides with one of the crystal axes.<sup>5,6</sup> In addition, the AMR was measured in the ferromagnetic phase at different current directions as a function of the field orientation, and the results were analyzed using an expansion allowed by the crystal symmetry.<sup>7,8</sup>

Here, we study the AMR and PHE of high-quality epitaxial thin films of SrRuO<sub>3</sub> for which other sources of magnetoresistance are relatively small. We study the AMR and PHE at 2 K for which the direction of the easy axis does not coincide with any of the crystal axes. In addition, we extract the direction of the magnetization which allows us to explore the dependencies of AMR and PHE on the orientation of the magnetization for various current directions. We find that a good description of

the behavior can be obtained by a minimal model consisting of three independent contributions related to: (a) the orientation of the magnetization relative to crystal axes, (b) the direction of the current relative to the crystal axes, and (c) the orientation of the magnetization relative to the current.

**II. SAMPLES AND EXPERIMENT**

Our samples are epitaxial thin films of SrRuO<sub>3</sub> grown on slightly miscut ( $\sim 2^\circ$ ) substrates of SrTiO<sub>3</sub> by reactive electron beam evaporation. The films are untwinned orthorhombic single crystals, with lattice parameters of  $a \cong 5.53$  Å,  $b \cong 5.57$  Å, and  $c \cong 7.85$  Å. The Curie temperature  $T_c$  of the films is  $\sim 150$  K, and they exhibit an intrinsic uniaxial magnetocrystalline anisotropy. Above  $T_c$  the easy axis is oriented along the  $b$  axis,  $45^\circ$  from the film normal.<sup>9</sup> Below  $T_c$  the easy axis exhibits a reorientation transition and the easy axis rotates in the (001) plane towards the film normal. At 2 K the angle between the easy axis and the  $b$  axis is  $\sim 15^\circ$  and the anisotropy field exceeds 7 T.<sup>10,11</sup> The data presented here are for a 27 nm thick film patterned to allow transverse and longitudinal resistivity measurements with different current directions relative to the crystal axes (see Fig. 1). The measurements are performed with PPMS-9 (Quantum Design).

**III. EXPERIMENTAL RESULTS**

In this report we study the dependence of the AMR and PHE on the magnetic orientation as it is rotated in the (001) plane. We identify the PHE resistivity ( $\rho_{xy}$ ) as the field-symmetric component of the transverse resistivity, extracted by exchanging voltage and current leads.<sup>12</sup> The measurements are performed at 2 K; therefore, we may assume that the magnitude of the magnetization is constant.

Figures 2 and 3 show  $\rho_{xx}$  and  $\rho_{xy}$  as a function of the angle  $\theta$  between the applied magnetic field and the film normal in the (001) plane. The data are shown for eight different in-plane current directions relative to the  $c$  axis and for three different fields. We observe a significant dependence on the magnitude of the applied field.

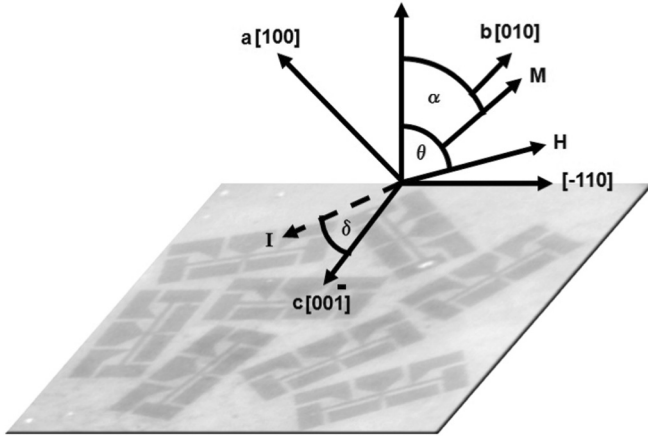


FIG. 1. A photo of the measured sample which consists of eight current directions and the definitions of the angles  $\alpha$ ,  $\theta$ , and  $\delta$ .

We expect the magnitude of the magnetization to be practically field independent; thus, we attribute this dependence primarily to the fact that the anisotropy field is larger than 7 T as a result of which, even for the highest applied field (8 T), the magnetization orientation is not expected to be parallel to the field and it depends on the field magnitude. However, we do not expect field dependence of  $\rho_{xx}$  and  $\rho_{xy}$  when plotted as a function of magnetic orientation.

To determine the orientation of the magnetization for given magnitude and orientation of the applied field, we use the Stoner-Wholfarth Hamiltonian which consists of a uniaxial anisotropy term and a Zeeman term:

$$\mathcal{H} = K_u \sin^2(\alpha - \alpha_{EA}) + M_s H \cos(\theta - \alpha), \quad (3)$$

where  $\alpha$  and  $\alpha_{EA}$  are the angles of the magnetization ( $M$ ) and the easy axis, respectively, relative to the film normal,  $K_u$  is the magnetocrystalline anisotropy constant, and  $M_s$  is the saturation magnetization. A certain choice of the anisotropy constant allows us to calculate the magnetization direction by minimizing the Hamiltonian. Using the anisotropy constant reported earlier<sup>11</sup> (corresponding to a 7 T anisotropy field) yields a good scaling of the longitudinal resistivity and PHE as a function of the calculated magnetization direction  $\alpha$ , which is shown in Fig. 4.

We note that for the patterns for which the average of  $\rho_{xx}$  over  $\alpha$  is higher, the scaling of  $\rho_{xx}$  with  $\alpha$  is less successful. On the other hand, the scaling of  $\rho_{xy}$  with  $\alpha$  is quite successful for all patterns. In principle, Lorentz magnetoresistance can induce deviations from scaling since it is related to the perpendicular component of the applied field and the same  $\alpha$  may correspond to different perpendicular components of the applied field. However, we would expect such an effect to be stronger when the resistivity is lower. Therefore, we believe that the deviations from scaling in  $\rho_{xx}$  for a given  $\alpha$  are related to negative magnetoresistance due to the suppression of magnetic disorder, which is expected to be larger in the more disordered patterns. Magnetic disorder is expected to yield an isotropic contribution to the scattering of the conduction electrons,<sup>13</sup> which does not contribute to the PHE.

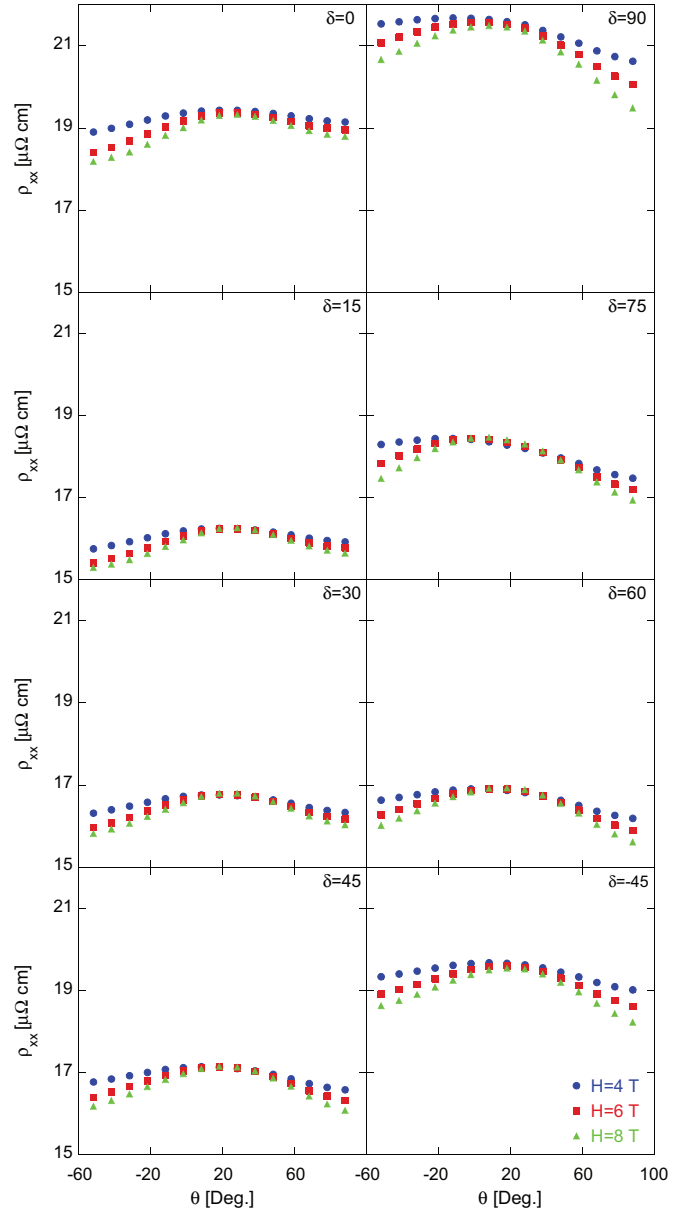


FIG. 2. (Color online) Longitudinal resistivity  $\rho_{xx}$  vs  $\theta$ , the angle of the applied field from the normal to the film.

The PHE for  $\delta = 0$  and  $\delta = 90$  is practically zero [see Fig. 4(a)] which suggests that [001] and  $[-110]$  directions are principle axes of the resistivity tensor projected on the sample plane (see Figure 1) consistent with previous reports.<sup>14</sup> We denote the resistivity along the [001] axis as  $\rho_1$  and the resistivity along the  $[-110]$  axis as  $\rho_2$  and  $\Delta\rho = \rho_2 - \rho_1$ .

We expect that for a given orientation of the magnetization

$$\rho_{xy} = \frac{1}{2} \Delta\rho \sin 2\delta \quad (4)$$

$$\rho_{xx} = \rho_1 + \Delta\rho \sin^2 \delta. \quad (5)$$

We expect two sources to contribute to the resistivity anisotropy ( $\Delta\rho$ ): a magnetic source and a crystalline source.

Using the results of Smit<sup>15</sup> that the principle axes of the magnetic contribution to the resistivity tensor are along the

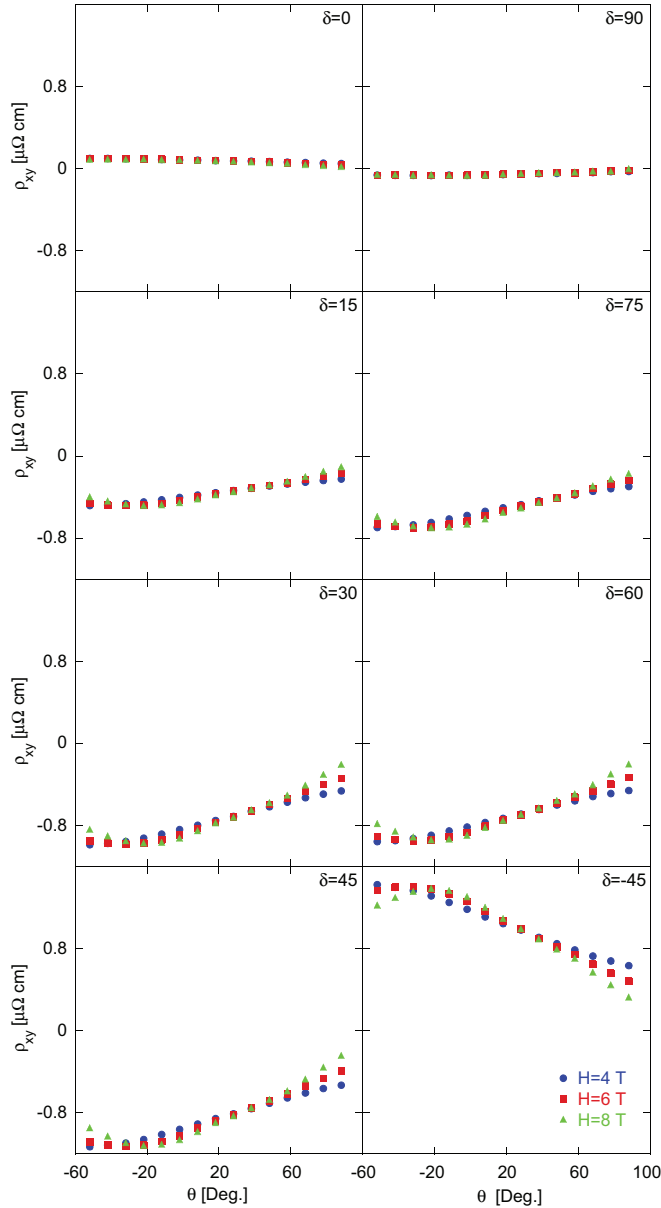


FIG. 3. (Color online) PHE resistivity  $\rho_{xy}$  vs  $\theta$ , the angle of the applied field from the normal to the film.

magnetization direction and the directions perpendicular to it, one can calculate the projection of the magnetic resistivity tensor on the measured plane for an arbitrary orientation of the magnetization. For magnetization which rotates in the (001) plane, the magnetic resistivity tensor has two in-plane principle axes along the [001] and  $[-110]$  axes. The magnetic contribution to  $\Delta\rho$  takes the form

$$\Delta\rho_{\text{Magnetic}} = \Delta\rho_M \sin^2 \alpha, \tag{6}$$

where  $\Delta\rho_M$  is a constant and  $\alpha$  is the angle between the magnetization and the film normal. We also expect  $\Delta\rho$  to include a constant contribution of a crystalline source which was measured previously, and was found to yield principle axes to the resistivity tensor that are along the [001] and  $[-110]$  axes<sup>14</sup> as also observed here. Combining the two sources

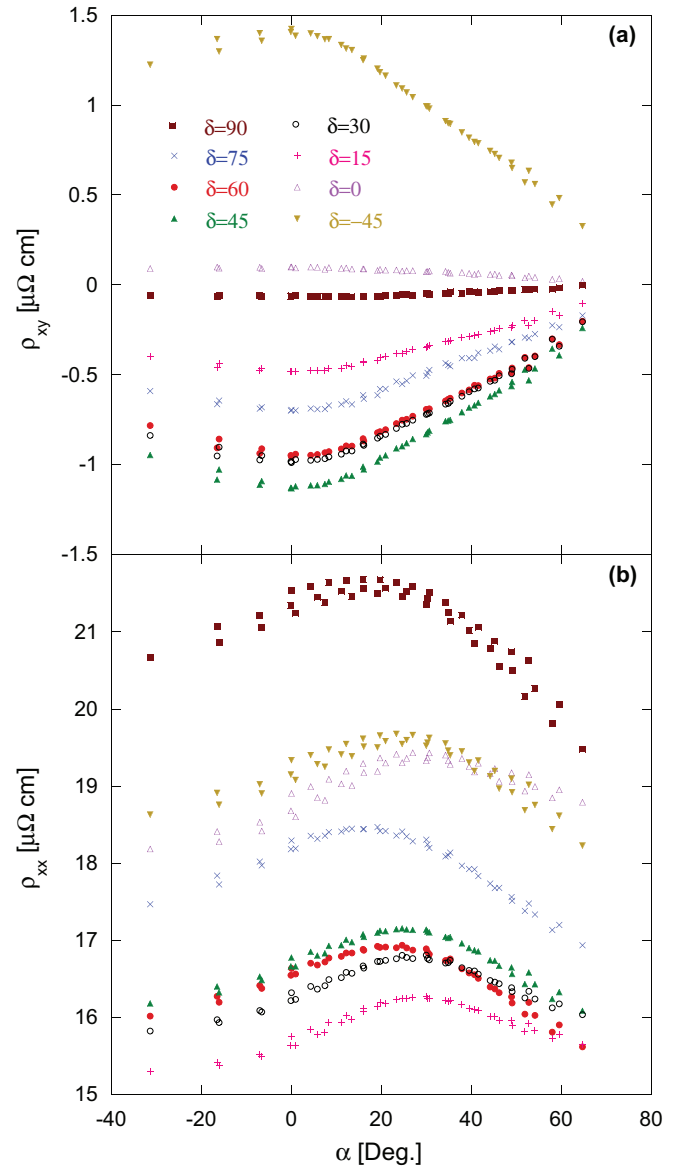


FIG. 4. (Color online)  $\rho_{xy}$  (a) and  $\rho_{xx}$  (b) vs  $\alpha$ , the calculated angle of the magnetization from the normal to the film.

together yields

$$\Delta\rho = \Delta\rho_M \sin^2 \alpha + \Delta\rho_{\text{crystal}}. \tag{7}$$

Thus combining Eqs. (4), (5), and (7) we have for our measuring configuration:

$$\rho_{xy} = -\sin \delta \cos \delta (\Delta\rho_{\text{crystal}} + \Delta\rho_M \sin^2 \alpha) \tag{8}$$

$$\rho_{xx} = \rho_c(\mathbf{M}) + \sin^2 \delta (\Delta\rho_{\text{crystal}} + \Delta\rho_M \sin^2 \alpha), \tag{9}$$

where  $\rho_c$  is the resistivity along the  $c$  axis. Excluding crystalline effects  $\rho_c$  is expected to be independent of the magnetization orientation as the magnetization rotates in the (001) plane perpendicular to the  $c$  axis; however, we note that  $\rho_{xx}$  for  $\delta = 0$  does depend on the magnetization direction [see Fig. 4(b)]. Such a dependence was previously measured in the paramagnetic phase and was shown to be a symmetric

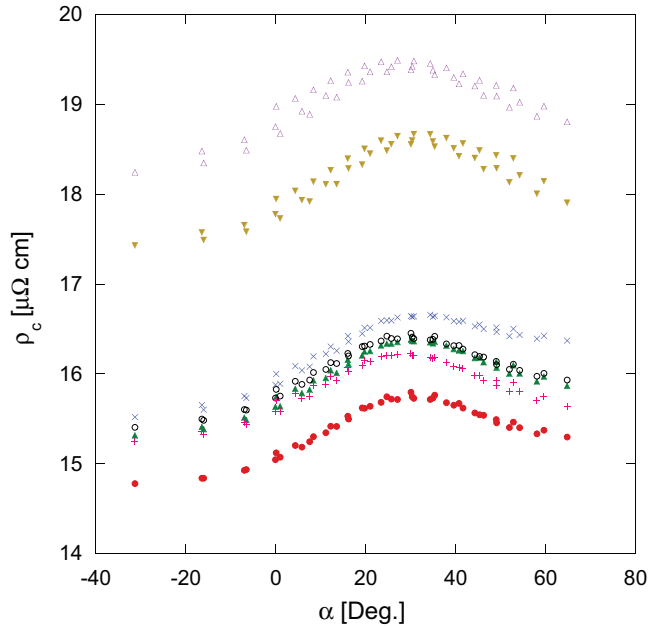


FIG. 5. (Color online) Extracted  $\rho_c$  vs  $\alpha$ , the calculated angle of the magnetization from the normal to the film.

function of the angle between the magnetization and the easy axis which coincides with the  $b$  axis, consistent with the system symmetry.<sup>6</sup> However, at 2 K there is an angle of 15 degrees between the easy axis and the  $b$  axis; therefore, we cannot expect such a symmetry to hold.

Equations (8) and (9) are supported by previous reports that found a behavior of the PHE and AMR consistent with this scenario.<sup>5,6,14</sup> To extract the dependence of  $\rho_c$  on  $\alpha$  we subtract from  $\rho_{xx}$  the angular dependent contribution  $\Delta\rho(\mathbf{M}) \sin^2 \delta$  which is equal to  $\rho_{xy} \tan \delta$ . The results for the different patterns are shown in Figure 5. We notice that  $\rho_c$  extracted for the different patterns has qualitatively the same dependence on  $\alpha$  up to a multiplicative factor. We attribute this factor to differences in the amount of disorder in the different patterns. Thus, to compare  $\rho_{xx}$  and  $\rho_{xy}$  of patterns with a different  $\delta$ , we normalize  $\rho_{xx}$  and  $\rho_{xy}$  for each pattern with  $\rho_c^0 \equiv \rho_c(\alpha = \alpha_{EA})$  extracted for this  $\delta$ . The normalized  $\rho_{xx}$  and  $\rho_{xy}$  are shown in Fig. 6.

Fitting the normalized  $\rho_{xy}$  with Eq. (8) yields a reasonably good fit for all of the patterns with  $\Delta\rho_M/\rho_c^0 \sim -0.13$  and  $\Delta\rho_{\text{crystal}}/\rho_c^0 \sim 0.14$  [see Fig. 6(a)]. Using the shape of  $\rho_c$  from Fig. 5 and plotting the expected normalized longitudinal resistivity based on Eq. (9) yields a good agreement with the data as can be seen in Fig. 6(b).

#### IV. CONCLUSIONS

We measured the low-temperature AMR and PHE for different magnetic fields and current directions and proposed a model which takes into account a combination of three decoupled contributions to the resistivity tensor which arise from structural and magnetic sources. We find that the behavior

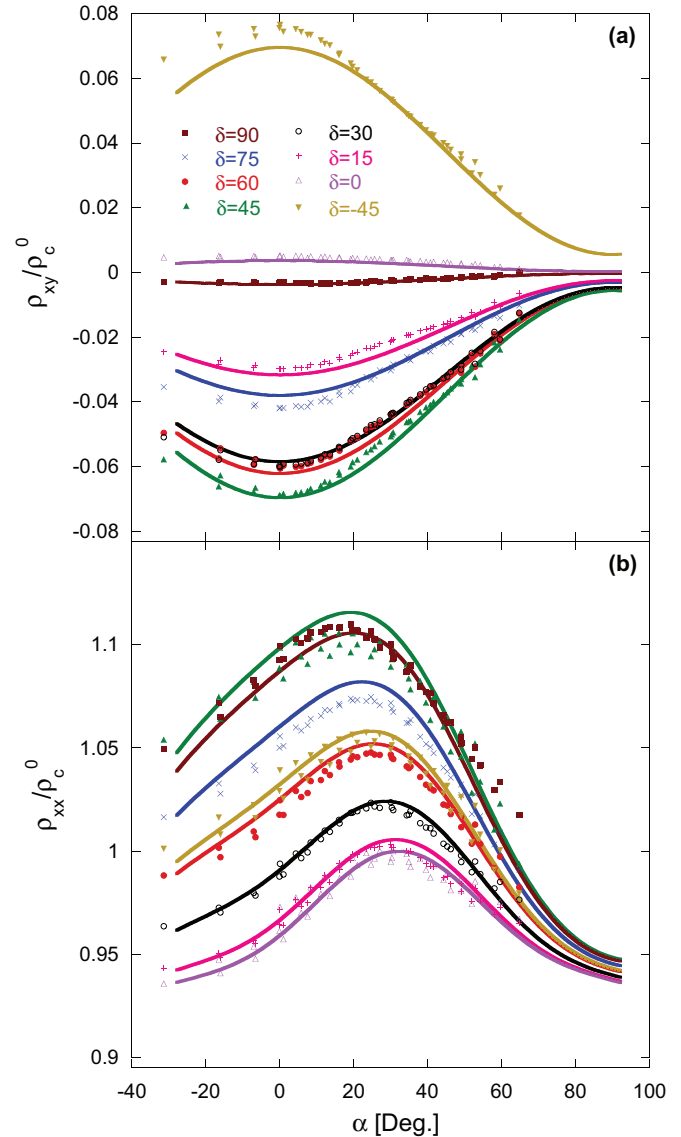


FIG. 6. (Color online)  $\rho_{xy}$  (a) and  $\rho_{xx}$  (b) normalized with  $\rho_c^0$  vs  $\alpha$ , the calculated angle of the magnetization from the normal to the film. The solid lines are fits to Eqs. (8) and (9).

of the AMR and the PHE can not be described by Eqs. (1) and (2). The PHE is described with a modified equation which takes into account the crystalline anisotropy source in addition to the common magnetic source. The AMR has a contribution which depends on the magnetization direction and is independent of in-plane current direction. In addition, it has the expected contributions which are present in the PHE resistivity.

#### ACKNOWLEDGMENTS

L.K. acknowledges support by the Israel Science Foundation founded by the Israel Academy of Sciences and Humanities. J.W.R. grew the samples at Stanford University in the laboratory of M. R. Beasley.

\*Contributed equally to this work.

- <sup>1</sup>T. R. McGuire and R. I. Potter, *IEEE Trans. Magn.* **11**, 1018 (1975).
- <sup>2</sup>W. Döring, *Ann. Phys.* **424**, 259 (1938).
- <sup>3</sup>Y. Bason, J. Hoffman, C. H. Ahn, and L. Klein, *Phys. Rev. B* **79**, 092406 (2009); N. Naftalis, Y. Bason, J. Hoffman, X. Hong, C. H. Ahn, and L. Klein, *J. Appl. Phys.* **106**, 023916 (2009).
- <sup>4</sup>G. Koster, L. Klein, W. Siemons, G. Rijnders, J. S. Dodge, C-B. Eom, D. H. A. Blank, and M. R. Beasley, *Rev. Mod. Phys.* **84**, 253 (2012).
- <sup>5</sup>Y. Shperber, I. Genish, J. W. Reiner, and L. Klein, *J. Appl. Phys.* **105**, 07B106 (2009).
- <sup>6</sup>I. Genish, L. Klein, J. W. Reiner, and M. R. Beasley, *J. Appl. Phys.* **95**, 6681 (2004).
- <sup>7</sup>M. Ziese, I. Vrejoiu, and D. Hesse, *Phys. Rev. B* **81**, 184418 (2010).
- <sup>8</sup>R. Gunnarsson, *Phys. Rev. B* **85**, 235409 (2012).
- <sup>9</sup>Y. Kats, I. Genish, L. Klein, J. W. Reiner, and M. R. Beasley, *Phys. Rev. B* **71**, 100403 (2005).
- <sup>10</sup>L. Klein, J. S. Dodge, C. H. Ahn, J. W. Reiner, L. Mieville, T. H. Geballe, M. R. Beasley, and A. Kapitulnik, *J. Phys.: Condens. Matter* **8**, 10111 (1996).
- <sup>11</sup>M. C. Langner, C. L. S. Kantner, Y. H. Chu, L. M. Martin, P. Yu, J. Seidel, R. Ramesh, and J. Orenstein, *Phys. Rev. Lett.* **102**, 177601 (2009); L. Landau, J. W. Reiner, and L. Klein, *J. Appl. Phys.* **111**, 07B901 (2012).
- <sup>12</sup>M. Büttiker, *IBM J. Res. Dev.* **32**, 317 (1988).
- <sup>13</sup>I. A. Campbell, A. Fert, and O. Jaoul, *J. Phys. C* **3**, S95 (1970).
- <sup>14</sup>I. Genish, L. Klein, J. W. Reiner, and M. R. Beasley, *Phys. Rev. B* **75**, 125108 (2007).
- <sup>15</sup>J. Smit, *Physica* **17**, 612 (1951).